24th European Rotorcraft Forum
Marseilles, France, 15th - 17th September 1998

Paper AC09

An Iso-Event Spanwise Interpolation Technique for Blade-Vortex Interaction Noise Prediction and Analysis

P. Spiegel

ONERA, Châtillon, France

This paper presents a method called Iso-Event Spanwise Interpolation (IESI). This method was developed for Blade-Vortex Interaction (BVI) noise predictions in order to reduce the required spanwise mesh density and consequently the computational time and memory. It contains an automatic analysis of the BVI events and simulates, at microphone position, the effects of the amplitude and phase continuity of BVI along span. As shown by a parametric study, the IESI reduces the number of required spanwise sections from 20 to about 6. It makes therefore more affordable the noise predictions using experimental blade-pressures measured either in flight or in wind tunnels. The IESI method can be generalized to other applications. The results of the analysis inside the IESI can be used to visualize the noise signature construction mechanisms and in particular to locate on the rotor disk the azimuthal and spanwise source extents at the origin of each peak on the acoustic signature. This possibility has already been used for low noise rotor design.

1. Introduction

The unique flight possibilities of helicopters make them potentially very attractive for many purposes, as well for civil as for military domains. However, this mean of transportation is not well accepted by people living near helicopter flight paths because of the noise it generates. Hence, continuing research effort has been pursued for several decades to reduce helicopter noise, in order to gain public acceptance, and thus to open new markets. Among all helicopter noise sources, the blade-vortex interaction (BVI) phenomenon, generated on the main rotor, remains one of the most annoying because of its impulsivity. It appears mainly in descent flight but can also be present in level flight.

Many research programmes have been devoted to the BVI noise reduction. They often consisted in an improvement of BVI noise prediction tools necessary for low noise rotor design. Experience showed that a reliable BVI noise prediction could be achieved only by accurate predictions of all the following variables and phenomena : rotor trim and dynamics, wake generation and convection, interacting-vortex roll-up, interacting-vortex strength and viscous-core evolution, unsteady blade pressures and resulting acoustics. One important concern of prediction code developers is to keep the computation time compatible with rotor optimization purposes.

This paper presents a method that saves computation time in the last or the two last steps of BVI noise predicition : the acoustic prediction using blade pressure data and possibly the blade pressure prediction itself. This method consists in an « intelligent » spanwise interpolation, called « iso-event spanwise interpolation » (IESI), that reduces the amount of blade pressure data required to achieve a given accuracy of noise prediction. Previous works were focused on spanwise blade pressure interpolation (starting from measured blade pressures) [1] in order to get the required amount of pressure data for noise computation, whereas the present method performs the interpolation directly on the acoustic signatures emitted by the blade sections for which pressure data are available. This present solution is faster than the previous one. It avoids the computation of the noise emitted by interpolated blade pressures.

A complementary way to reduce the blade optimization process cost and duration is to reduce the amount of blind parametric studies. This requires a good understanding of the noise generation mechanisms and their dependence on the design parameters. The IESI technique consists partly in analyzing the links between BVI events and the resulting pressure peaks in the acoustic signatures. Hence, the available information is provided to the user and helps him to understand the noise signature construction and to guide blade optimizations. For example, the azimuthal and spanwise extent of BVI responsible for each acoustic pressure peak can be identified and the acoustic effect of a sweep in the blade planform can be shown and somehow predicted.

This paper explains the IESI technique, after a brief presentation of the acoustic code in which it has been implemented. Then, the improvements obtained on acoustic predictions are shown on acoustic signatures and on noise contours through a parametric study on the number of blade sections serving for the computation. The possible tools for the analysis of the BVI acoustic signature construction are also presented.

2. The Iso-Event Spanwise Interpolation (IESI) technique for BVI

Background : the PARIS code

General description

This code, described in details in [2], is based on the Ffowcs-Williams and Hawkings (FW-H) equation. It uses a time domain formulation to predict thickness and loading noise. A first version of this code was presented in [3].

The loading noise can either be performed in compact sources or in non-compact sources. The blades are assumed to be stiff. The rotor is fully articulated with an arbitrary periodic motion. All blades are assumed to have the same geometry, the same motion and the same loads.

The code was mainly validated in the framework of the HART cooperation [4]. Besides the comparison of predictions to experiment, the HART Prediction Team members also compared their respective acoustic codes using the same inputs, on complete rotor cases [5] and on 24 simple cases taken from an appendix of [2]. These cases concern only one blade surface panel but cover the main parameter variations. WOPWOP [6] and PARIS provided exactly the same results, for thickness and loading noise, on all 24 cases.

Features

Whereas most of the codes based on the FW-H equations are direct applications of Farassat's formulations [7], the PARIS code is built in a different manner. The equations are written in a frame fixed with respect to the helicopter, in their convected form, mainly because everything is periodic in this frame. The calculation are performed starting from the emission times [3] and not from prescribed reception times. This avoids to solve the retarded time equation, as the microphones are supposed fixed in the helicopter frame. It also provides a self-adapted reception-time step :

- The constant emission time step used for thickness noise calculation leads to an automatic concentration of the reception times during the negative acoustic pressure pulse, through Doppler effect.
- If the loads are given with variable time steps, with a concentration of points during BVI for example, the loading noise time steps at reception time will automatically follow these variations, in addition to the background variation due to the Doppler effect.

This provides optimized time steps in the calculation as well as in the results.

Another contribution to the reduction of computer time, is the use of two different time steps for the terms varying slowly versus azimuth, like the thickness noise terms and the Green's function terms, on the one hand, and for loading noise terms (BVI) on the other hand. The first one is a constant 2 degrees azimuthal step (180 azimuths) whereas the second is varying between 0.2 degree and 3 degrees (usually 1000 azimuths or more). The slowly varying terms needed for loading noise computation are then interpolated at the loading noise calculation azimuths.

The CPU time of PARIS is about 0.9 s per microphone position on a Cray C98/5-216 for thickness plus BVI noise computations. An estimation presented in [2] suggests that PARIS needs about 40 times less CPU time than WOPWOP.

The major innovations in the PARIS code are the methods described hereafter and mainly developed for BVI noise computations. Their development started in 1991 [3] and was quite completed in 1995 [2].

Overview of the IESI technique for BVI noise calculation

Failure of a conventional spanwise integration

Let us consider two spanwise blade sections located at Radii r_1 and r_2 for which noise signatures have been calculated. The objective is to compute the loading noise emitted by the blade extent between r_1 and r_2 (Fig. 1). When these radial locations are far from each other, the simple spanwise integration consisting in the addition of the noise signatures emitted at r_1 and r_2 and weighted by the half spanwise extent, fails as shown on Fig. 1. On this figure, the plot on the top right shows how BVI acoustic Pulses c_1 and c_2 resulting respectively from the interaction of Sections r_1 and r_2 with the same vortex c, are out of phase. The phase difference can be caused by different emission times (non-parallel BVI) or by different propagation distances (microphone not perpendicular to the BVI location line). The plot at the bottom of Fig. 1 shows the difference between the weighted addition of these signatures, and the actual one. The first leads to two sharp peaks, whereas the actual one consists in one smooth peak only. The actual phenomenon is an interference effect of all the signatures emitted by intermediate sections, the positive peak associated to a given section being partly cancelled by the simultaneous negative peaks of the neighbouring sections.

Note that on Fig. 1, the signatures of sections r_1 and r_2 are not given in term of acoustic pressure but in term of spanwise derivative of the acoustic pressure. The signature of the whole blade can then be considered as the spanwise integration of the spanwise derivative of the acoustic pressure signature.

Principle of the IESI

The method presented here consists in the generation of intermediate section signatures starting from the known signatures of Sections r_1 and r_2, in order to simulate the actual interference effect. The starting point idea is to use the fact that the governing parameters of BVI noise generation vary continuously along span (vortex characteristics, blade geometry, blade velocity...). Consequently, there is also a continuous variation of the signature emitted by an interacting blade section, when this section is moved from r_1 to r_2. This variation mainly consists in amplitude and phase shifts of the acoustic pressure peak emitted by each BVI, and secondarily in a small change in shape of these peaks. The IESI technique illustrated on Fig. 2 is a simple mean to simulate these shifts. A ruled surface is generated in a 3D space with axes of coordinates respectively corresponding to the reception time, the emission radius and the acoustic pressure spanwise derivative. This surface is obtained by the motion of a straight line that follows simultaneously the signatures of Sections r_1 and r_2. This line crosses simultaneously the peaks due to a same interaction on both signatures : it links Point c_1 and c_2 for example. Note that the line does not remain parallel to itself during such a motion because the phase shift of the linked BVI pressure peaks varies from one BVI to the other. The intersection of the ruled surface with a plane at r provides an approximation of the signature emitted by the blade section at radius r.

The interpolated signature obtained is only an approximation because the amplitude and the phase of each BVI peak may not vary exactly linearly between the two sections, for several reasons (vortex curvature, blade curvature...). It has been verified, however, that such an approximation is valid as long as Sections r_1 and r_2 are not too far from each other (let's say 0,1 blade radius).

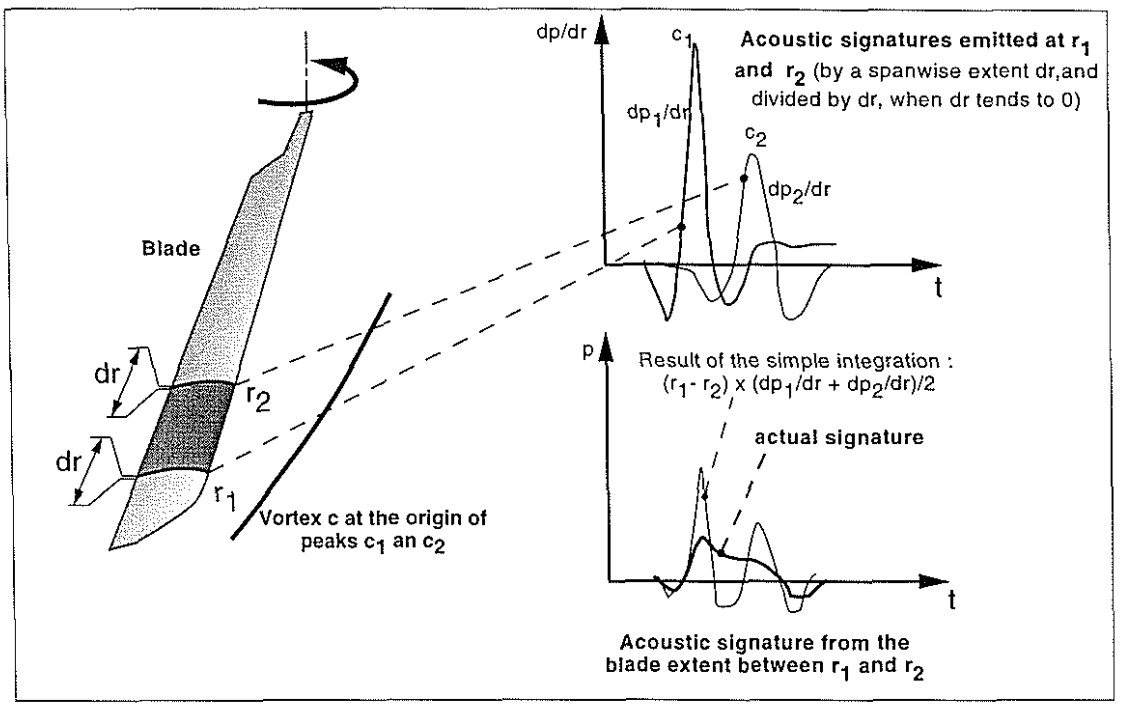

Fig. 1. Failure of the simple integration of the noise emitted by the blade extent comprised between r_1 and r_2 when this extent becomes too large.

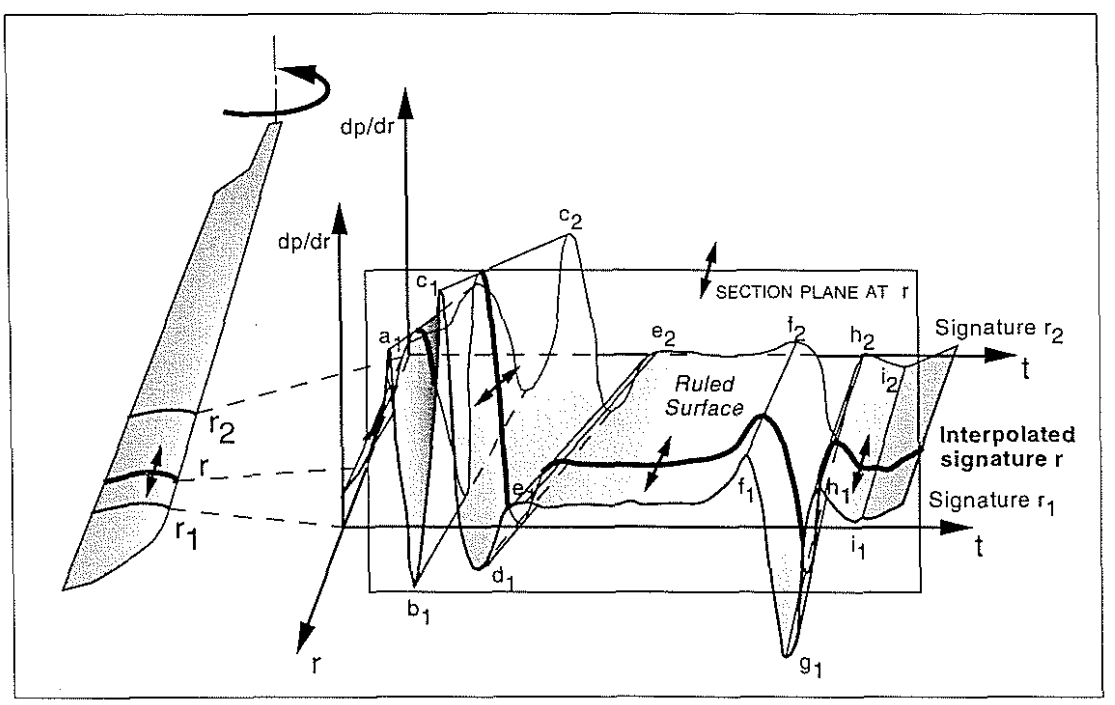

Fig. 2. Principle of the iso-event spanwise interpolation technique of acoustic signatures.

The principle applied for one section r can be applied to as many sections as required. The corresponding signatures can then be weighted by their spanwise extent and added. This operation is equivalent to a spanwise integration of the ruled surface at each reception time.

Further explanations on the steps of the construction of the ruled surface are given hereafter.

Research of the dominant peaks on a blade-section acoustic signature

The research of BVI peaks on the signatures r_1 and r_2 leading to the ruled surface definition is only performed in the reception time windows corresponding to the azimuthal area of possible noisy BVI. First the relative maxima and minima of the signatures are identified. The shape of each relative peak is then analyzed. A value called « strength » is then assigned to each peak, increasing with the value of the pressure at the peak, the relative height and the width of the

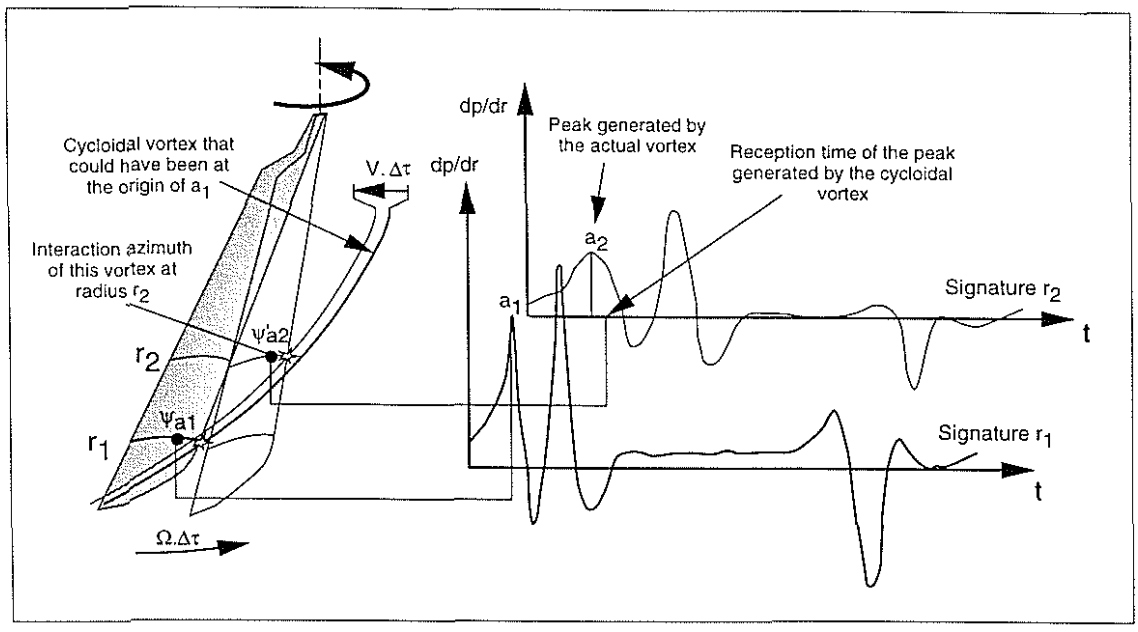

Fig. 3. Use of the cycloidal vortex model to link the peaks of signatures r_1 and r_2 coming from a same actual vortex.

peak. The sign of the strength function is the same as the one of the pressure. Only the 15 strongest peaks are kept, in order to avoid wasting time in applying the following procedures to poorly significant information.

Link of the peaks with those of the following section

The next step in the method consists in finding the links between the peaks selected on the signatures of r_1 and r_2, Note that for real acoustic signatures which contain many BVI peaks, these links are not as obvious to find as on the simplified example of Fig. 2. Hence, complementary information on the BVI positions on the rotor disk are needed. The BVI positions could be read in data files provided by the aerodynamic code that computes the blade pressure data. However the solution consisting in guessing the BVI positions by comparing a background model of BVI geometry to the analysis of the signatures was preferred because of its autonomy : no adaptation of existing aerodynamic codes are needed and the method works also with measured blade pressures even when additional information on vortex positions are not available.

The model of BVI geometry used is the simplest one : the cycloidal vortex. Only the projection on the rotor disk is needed here because the perpendicular-to-disk position plays no role in the phase of BVI. Fig. 3 shows how this cycloid model is used for finding the peak to link with Peak a_1. The reception time of a_1 permits to deduce the blade azimuth at interaction time, ψ_{a1}, assuming the leading edge is the noise source of the whole section signature. A cycloidal vortex crossing the leading edge at this time is then built. The interaction time of this vortex with Section r_2 is found assuming that this vortex is convected at the unperturbed upstream velocity V. The corresponding reception time on Signature r_2 is deduced using again the leading edge noise source model. The peak on Signature r_2 to link with a_1 is then chosen among the previously selected peaks. This choice is made by comparing the reception time of these peaks to the reception time of the cycloidal vortex interaction, and by comparing their strength to the strength of Peak a_1. In case the comparisons are too bad, no link with a peak of Signature r_2 is made.

Note that the built cycloidal vortex is not necessarily considered as emitted at a blade tip, as actual vortices are not.

Event function for the two considered sections

The orientation of the straight line describing the ruled surface must be defined all over the reception time period and not only for linked peaks.

Therefore an event function is created for Signature r_1 and for Signature r_2. The straight line must then always link points on both signatures having the same event value. The event must be an increasing parameter versus reception time, hence versus emission azimuth. For Signature r_1 it is arbitrary chosen as the emission azimuth. Fig. 4 shows how it is deduced for Signature r_2, The two event values must be the same for two linked peaks. Between these known values the r_2 event function is linearly interpolated as a function of emission azimuth. At $\psi = 0$ and $\psi = \pi$, the event on r_2 is the same as on r_1 so that the interpolation direction on rotor disks stays close to radial in areas where no noisy BVI occur (Fig. 5).

Construction of the signature of the blade part between the considered sections

The signature of the intermediate sections between r_1 and r_2 are computed using the motion of the straight line following the signatures of r_1 and r_2 with a simultaneous event function variation from 0 to 2π. These signatures are then all expressed at same reception times, weighted by their spanwise extent and added to provide the integrated signature of the blade extent between r_1 and r_2.

The number of intermediate sections to consider between r_1 and r_2 is determined to be consistent with the local time step along the signatures and the direction of interpolation on the ruled surface. An oblique interpolation converts a spanwise step into a time step which must not be greater than the time steps of the interpolated signatures.

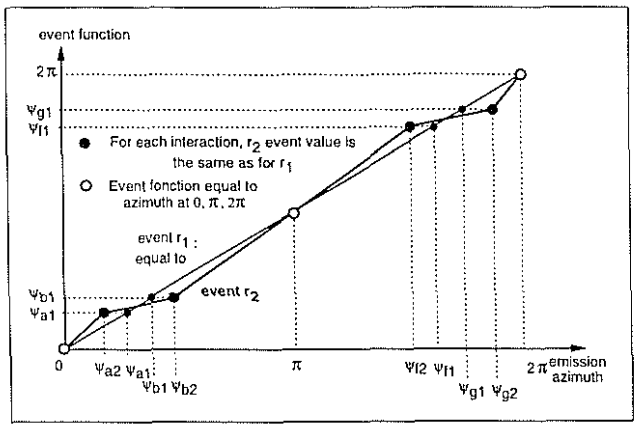

Fig. 4. Deduction of r_2 event function from the associated events between r_1 and r_2.

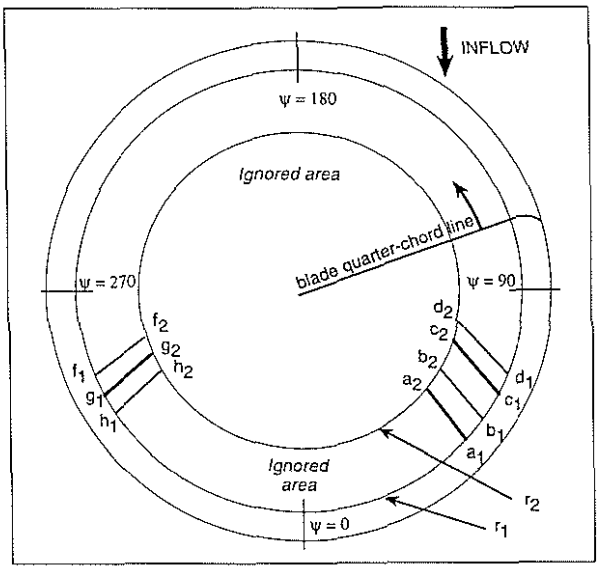

Fig. 5. Peak associations seen on the rotor disk.

Remark 1 : possible options

In the IESI implemented in the PARIS code, the peak association using the cycloid vortex model is repeated for each microphone position. An improvement for noise contour plot computations would consist in doing this association once for all microphones by analyzing the blade pressure (or lift) time derivatives rather than the acoustic signatures.

Other improvements could consist in replacing the linear interpolation leading to the ruled surface by non-linear interpolations. The vortex and blade curvatures could be taken into account in the interpolated phase, and the non-linear acoustic response along span could be taken into account in the interpolated amplitude.

Remark 2 : application to other fields

The IESI technique developed for BVI noise can also be applied to thickness noise in order to interpolate the negative acoustic pulse emitted by each section. This is done in the PARIS code in which the event function for thickness noise is simply taken equal to the quarter-chord azimuth at emission time.

It could also be applied to High Speed Impulsive Noise (HSI) calculations, allowing the use of a coarse spanwise mesh in the shock area whereas up to now dense meshes were used. The event in this case would be the shock pressure pulse. The peak associations in the acoustic signatures would be much simpler than in the case of BVI because the generating event in this case (the shock) is unique.

The background philosophy of the IESI, consisting in interpolating in a direction of slow variation of a physical quantity, can be generalized for other events and variables than respectively the BVI and the span. For example, in [8], the quantity followed is the acoustic pulse emitted at one emission time by a Kirchhoff-surface panel (of a rotating mesh). The variable concerned by interpolation, which is the radius r in the IESI (Fig. 2), is here the emission time τ. The ruled surface is built by linking the different pulses coming from the same panel and emitted at different emission times (as on Fig. 2 for BVI pulses). This « iso-panel timewise» interpolation allows to use large emission time steps in the computation of the signature of each panel, when the panel emission varies slowly, as for instance in the case of HSI noise of a hovering rotor. Note that, the dp/dr derivative used for the integration over r after the IESI is replaced here by the $dp/d\tau$ derivative (called rate of pressure in [8]) for the integration over emission time τ.

3. Effect of the IESI on BVI noise calculations

Many calculations were performed using the PARIS code in order to validate the behaviour of the iso-event interpolation and assess its interest. Each calculation was performed twice, with iso-event interpolation and without.

Computation chain providing aerodynamic input data

The aerodynamic blade pressures used as input data for the PARIS code were computed using the ONERA computation chain for BVI calculations [9]. A first code computes the rotor trim (R85/METAR [10]). It takes into account aerodynamic, inertial and elastic forces and moments on the blade. It contains a vortex-lattice wake model the geometry of which is prescribed depending on the rotor trim. This wake is then distorted using a free-wake analysis (code MESIR [11]), assuming that distorting the wake does not significantly change the rotor trim. The results of the free-wake analysis are used in a wake roll-up model (code MENTHE [12]) in order to find the location and circulation of the interacting vortices. The interaction of these rolled-up vortices with the blades is then computed using a code based on a singularity method and including a cloud vortex model for close interactions (ARHIS [13]), in order to provide the unsteady blade pressures required for acoustic calculations. The first codes use coarse azimuthal steps (about 10 deg.) whereas the blade pressure are computed with a small and variable azimuthal step depending on the vortex position relative to the blade (between 0.2 deg. and 3 deg.).

Computation conditions : HART tests

The BVI conditions for the computation were taken from the test matrix of the HART campaign [4]. The widely published cases called Baseline, Minimum Vibration and Minimum Noise were selected. These cases simulate 6-deg.

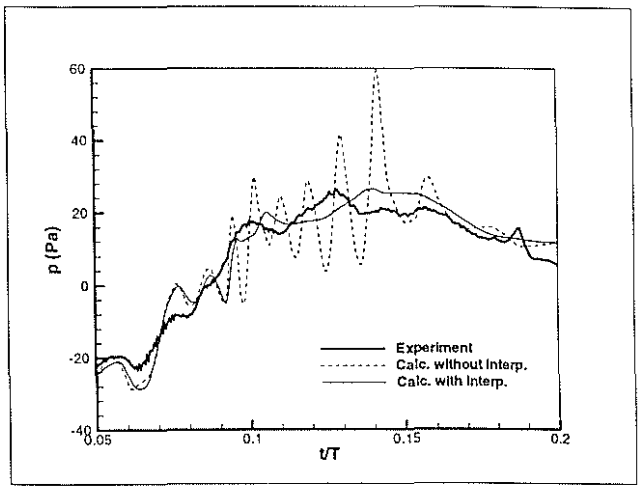

Fig. 6. Elimination by the IESI of non-physical peaks of the computed acoustic signature.

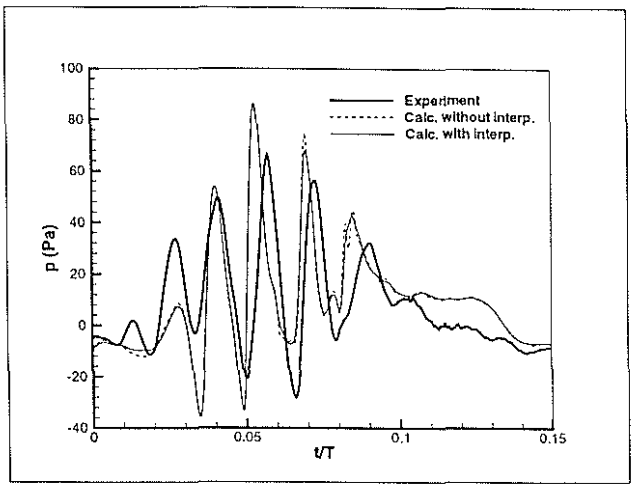

Fig. 7. The IESI keeps physical peaks of the computed acoustic signature.

descent flight conditions for an advance ratio $\mu = 0.15$, $C_T = 0.0044$, $\alpha_{shaft} = 5.3$ deg., and $\alpha_{TPP} = 3.8$ deg. The first case has only a monocyclic control law whereas in the two others a 3/revolution Higher Harmonic Control component is added with two different phases.

The test rotor was a 40% dynamically scaled model of a BO105 rotor. Its main characteristics are the following : four blades, 2 m radius, 0.121 m chord length, rectangular planform, -8 deg. linear twist (root to tip), 2.5 deg. precone angle, modified NACA 23012 airfoil, and 1050 rpm rotor nominal operating speed. The rotor is rotating counter-clockwise (viewed from above).

Effect on signatures in agreement with physics

The correct reproduction by the IESI of the interference effect suggested in Fig. 1 can now be checked. This effect occurs mainly for sidewards microphones because the phase shifts between the signatures coming from each section are the highest. The microphone position chosen here is 2.3 m below the rotor, 2.7 m on the advancing side (Microphone 11 on the DNW array [4]), and 0.5 m upstream the rotor center. The PARIS calculation was performed with 10 blade sections (plus tip). Fig. 6 (in which T is the rotor revolution period) shows, in the Minimum Noise case, how the IESI cancels the spurious peaks of the signature obtained without IESI and coming from each section. The signature obtained with IESI is close to the measured one.

Fig. 7 shows the computations on the same microphone but for the Minimum Vibration case. For these case many peaks are present on the measured signature. The IESI method does not cancel the corresponding predicted peaks. The interference is constructive as the contribution of the signatures coming from the intermediate sections are in phase. The results of Figs. 6 and 7 could not have been obtained by a simple filtering of the signatures : a filtering could indeed cancel the peaks of Fig. 6 but it would then also cancel those of Fig. 7.

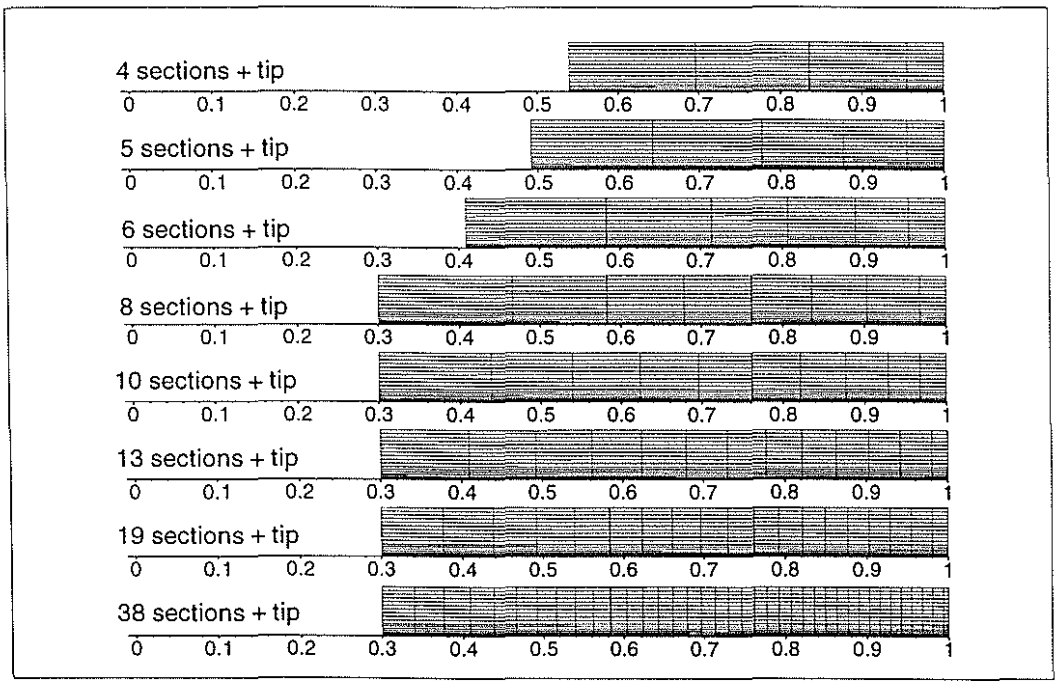

Fig. 8. Blade spanwise discretizations used for the parametric study on the IESI benefits (abscissa : relative radius).

Accuracy versus the number of computed blade sections

A parametric study was performed in order to observe the effect on the acoustic predictions of the number of blade sections used in the calculation, with and without IESI.

The aerodynamic pressure were computed by ARHIS on 38 blade sections. Blades with less sections, from 4 to 19, were generated by selecting sections among the 38 computed, as shown on Fig. 8.

Noise contour plots like those generated during the HART tests in DNW mainly concern quite near-field positions and the directions of maximum noise radiation. However for the certification cases or for fly-over cases, a good prediction accuracy must also be achieved in far field and in more lateral directions. Furthermore, for noise abatement flight procedure optimizations, it is also important to provide accurate predictions in directions up to the rotor plane. Indeed, during maneuver flights, areas on the ground can be located in the rotor plane. Therefore, a new kind of noise contour plots is proposed on Fig. 9. It concerns far field positions corresponding to certification distances and to a full scale rotor (10 m diameter). The part of plane 120 m below the rotor reproduces a rectangular area located between the certification microphones (150 m on each side). The part of sphere centered on the rotor is tangent to the lateral certification microphone lines. It is split in two parts, left and right, and each part is placed in the same plane than the previous rectangular noise contour plot, like for a Mercator planisphere. The transformation applied to the sphere leaves unchanged the surface area of each panel.

Fig. 10 presents the noise contours computed for the Minimum Noise case, using the type of plots previously presented. The noise levels correspond to the frequency range going from the 6th to the 40th blade passage frequency. Note that a color increment in the scale represents 3 dB, which is a large value when it is used in an optimization process. The reference calculation, using 38 blade sections and without IESI, is shown at the top left of the figure. The calculations using 38 sections with IESI provides the same result. For 10 sections and below the differences become large. The calculation without IESI tends to highly overpredict noise levels whereas the calculation with IESI stays close to the result obtained with 38 sections. The maximum noise level obtained with 38 sections is 84.1 dB. With 4 sections, the maximum is 3.6 dB higher without IESI, and only 0.5 dB lower with IESI.

The differences are even much higher on other directions than those of maximum radiation, as show on Fig. 11. On this figure the noise contours represent the absolute value of the difference of noise levels between each calculation and the reference calculation with 38 sections. The calculation with IESI tends to underpredict the noise in the forward direction on the retreating blade side, when the number of computation sections is reduced. The calculation without IESI tends to highly overpredict the noise levels on the advancing side and near the rotor plane (more than 8 dB with 4 computation sections).

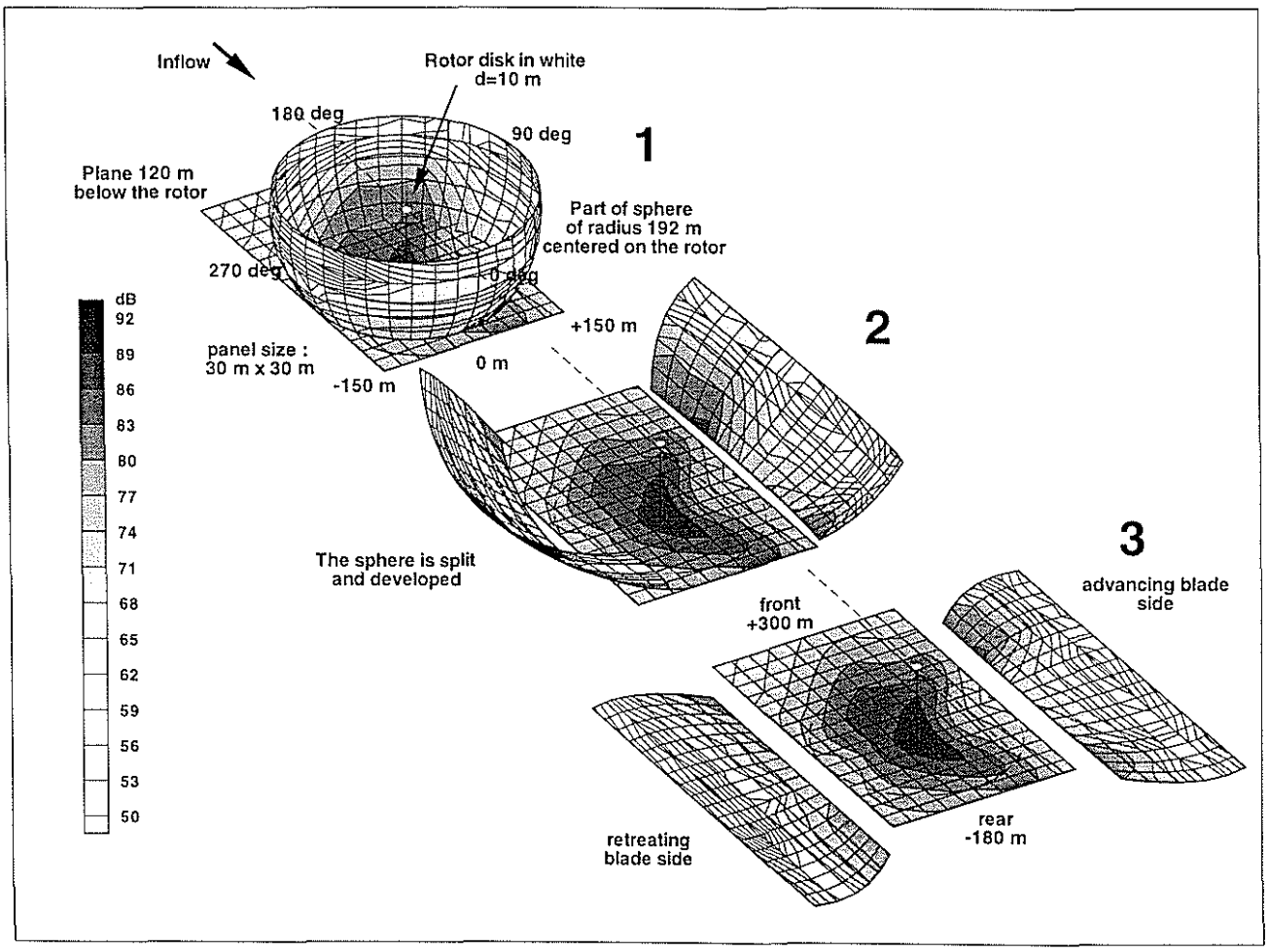

Fig. 9. Geometry of wide angle noise contour plots (HART Baseline case).

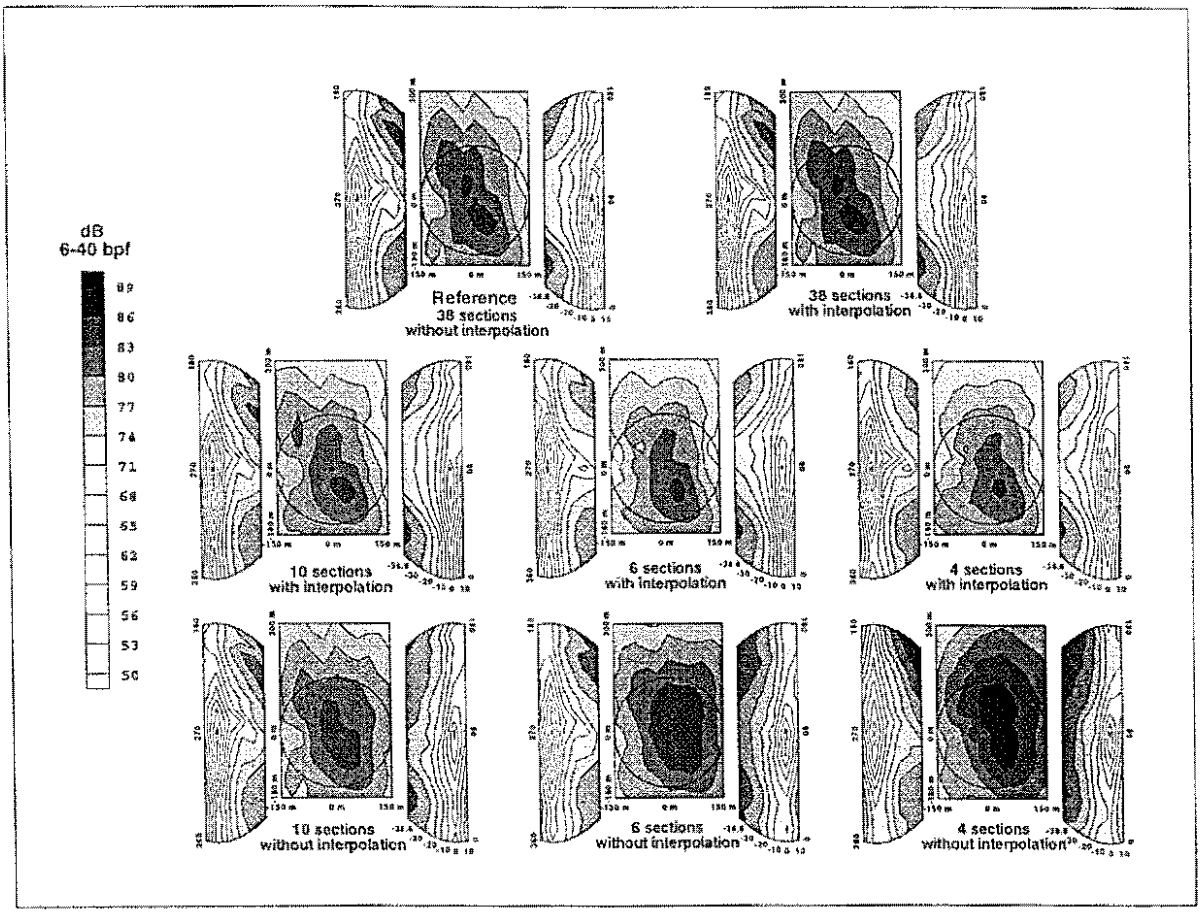

Fig. 10. Effect of the number of blade sections on noise predictions, with and without spanwise interpolation. Minimum Noise case.

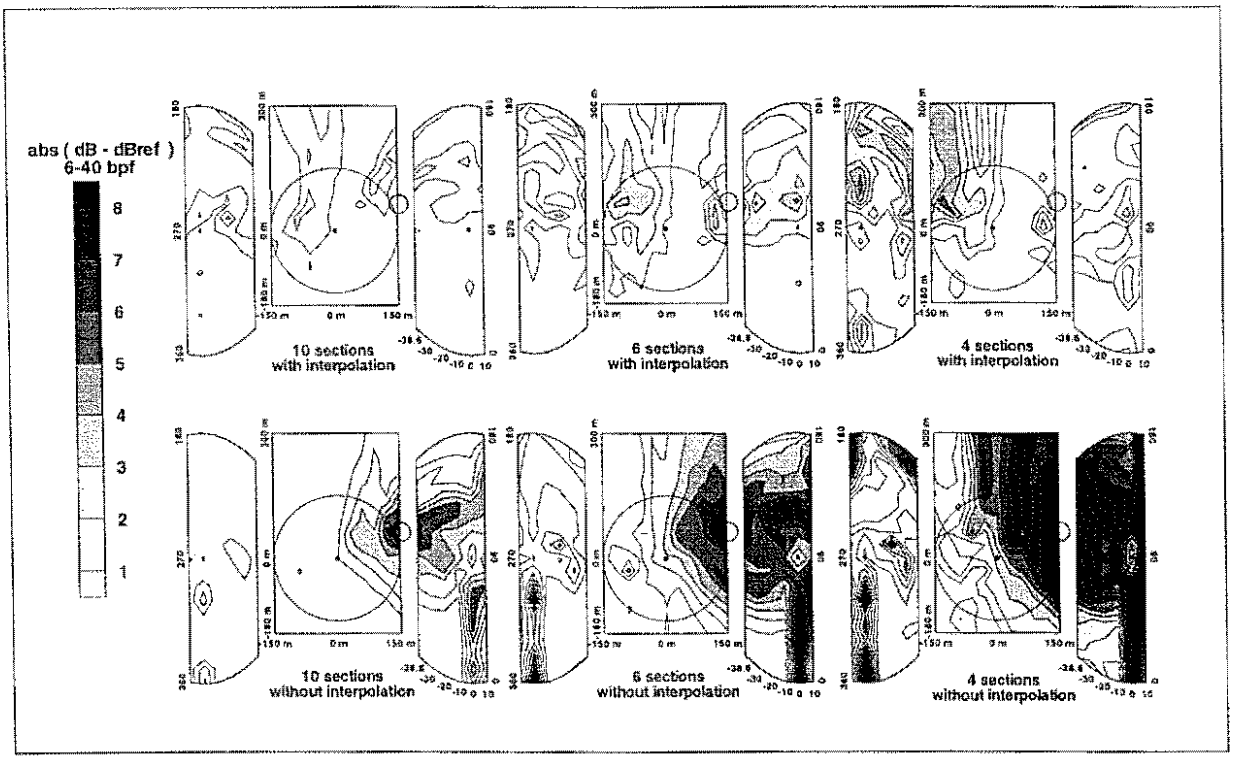

Fig. 11. Difference with the noise levels computed using 38 blade sections (reference.). Minimum Noise case.

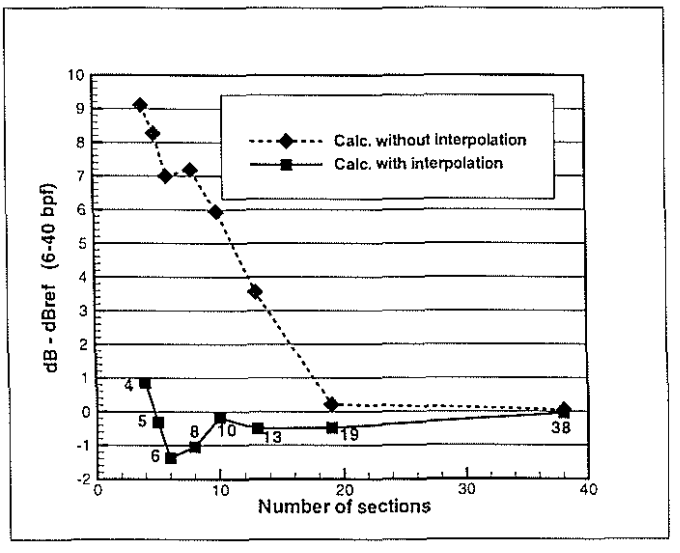

Fig. 12. Convergence of noise levels at circled point of Fig. 11.

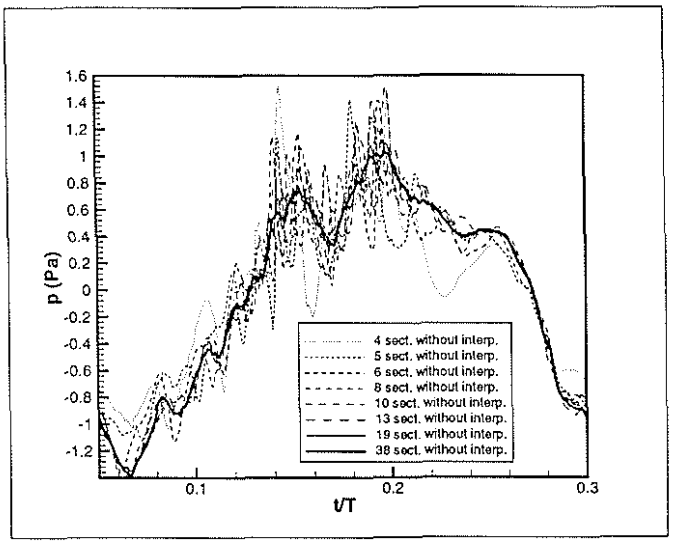

Fig. 13. Convergence of acoustic signatures without IESI.

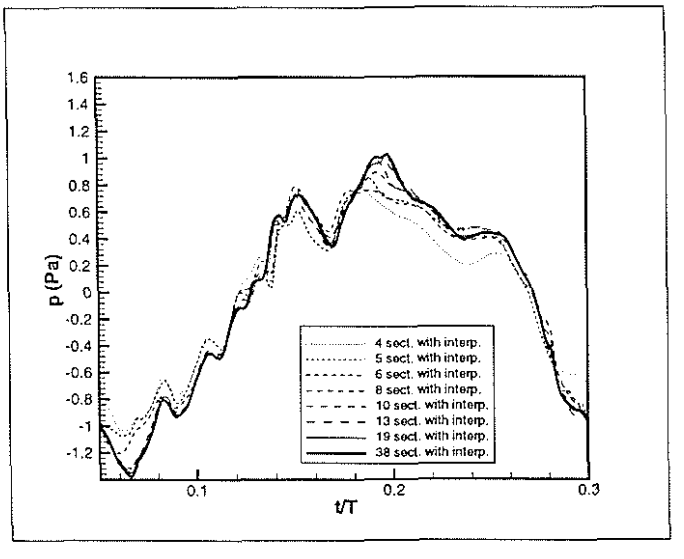

Fig. 14. Convergence of acoustic signatures with IESI.

The position of highest overprediction on the certification microphone lines is shown by a small circle on the contour plots of Fig. 11. It is located 150 m on the advancing side and 60 m upstream the rotor center. Fig. 12 shows the evolution of the noise levels predicted at this point as a function of the number of computation sections with and without IESI. Without IESI 19 sections are necessary to obtain a correct accuracy. This is in agreement with [14] where the minimum number of sections has been found between 15 and 20. With IESI, 10 sections are sufficient and even less if 1 dB accuracy is enough. Figs. 13 and 14 show the evolution of the computed noise signatures at this point respectively without IESI and with IESI. On Fig. 13, it is clear that the predicted peaks have no physical origin as their number and positions vary with the number of computation sections. Fig. 14 shows the robustness of predictions with IESI.

The same figures as Fig. 13 and 14, but for the microphone position 300 m upstream the rotor center and 150 m on the retreating side would show that the correct noise level found without IESI is a hazard because the signatures obtained with 4 sections and with 38 sections are very different. The underestimation of the predicted noise level with IESI and with 4 sections, at this position (see Figs. 10 and 11), is due to the error introduced by the use of linear amplitude and phase interpolations for very distant blade sections (see Remark 1).

Since the effect of the IESI is the most important for low noise level predictions, this could lead to the conclusion that IESI presents a weak interest. However, it is important to correctly predict low levels for rotor optimizations, for at least two reasons :

- The comparison of maximum noise levels of different flight cases must be correct and therefore the low noise cases must also be well predicted. For example, the actual maximum-noise-level reduction obtained in the Minimum Noise case of the HART campaign, compared to the Baseline case, is predicted as a noise increase when the number of sections is reduced, without IESI.
- It is important for annoyance evaluation or certification simulations that the noise be also well predicted elsewhere than in the direction of maximum radiation. For example, the noise levels used for certification on the advancing side are overestimated by 5 dB for the Minimum Noise case, using 10 computation sections without IESI, whereas the maximum level is correct.

The reduction of the number of sections to serve for the computation thanks to the use of IESI depends on the microphone position and on the flight case. It could be said that the IESI reduces by a factor 3 the number of sections required to guaranty a given accuracy in all directions. This reduction not only concerns the acoustic computations, but also the blade pressure computations and the memory needed to store pressure data files. Hence, the CPU time of the ARHIS and PARIS code are reduced by a factor about 3. On a Cray C98/5-256, PARIS needs 470 s CPU time to compute a thickness+loading noise contour plot on 415 microphone positions like the one presented on Fig. 9, with a 10 sections blade and with IESI.

The IESI avoids automatically the construction of spurious pressure peaks due to a too coarse spanwise mesh. Therefore, even if the gain achieved by IESI concerning the reduction of the number of sections is not always well known, it is interesting to know that with 10 sections the computation is always reliable, for a quite rectangular blade. For irregularly shaped blades, the number of required sections may sometimes be larger than 10, as the discretization must be sufficient to describe all aerodynamic variations along the span.

Interest for noise computations using measured blade pressures

The noise prediction using measured pressures becomes more affordable using the IESI because the number of pressure sensors to install on blades is reduced, and so is the number of channels of the acquisition system. Such noise predictions could be helpful to simulate and optimize noise abatement flight procedures starting from pressure measurements in a series of flight conditions. They could also be used for noise predictions of instrumented model rotor tested in wind tunnels, even if these wind tunnels are not anechoic. These predictions could provide the full scale fly-over noise radiated on the ground starting from pressures measured on the wind-tunnel model.

4. A derived tool for BVI analysis

Types of plots and data

The information available from the analysis required by the IESI, such as peak associations, correlation between reception time and emission position are made available through an output file of the PARIS code. Furthermore plots like those in Fig. 15 can be obtained from another file containing also detailed signatures. Fig. 15 concerns a microphone position from the wide angle noise contour plots (Fig. 9), located 120 m below and 150 m upstream the rotor. The flight conditions are those of the HART Baseline case (as in Fig. 9).

The top of Fig. 15 shows the ruled surfaces presented in Fig. 2, seen from the top, as defined automatically by the IESI. The loading noise signature is given in the same time frame as the ruled surfaces, as well as the thickness and loading noise of the whole (4 bladed) rotor, which mainly consists here in the addition of 4 loading noise signatures evenly delayed. The Y-axis for the signatures is the pressure and not the radius (superimposed plots). Vertical lines are plotted starting from a selection of peaks of the loading noise signature. The lines are solid for positive peaks, corresponding to the clear colors on the ruled surface. They are dotted for negative peaks, corresponding to dark colors.

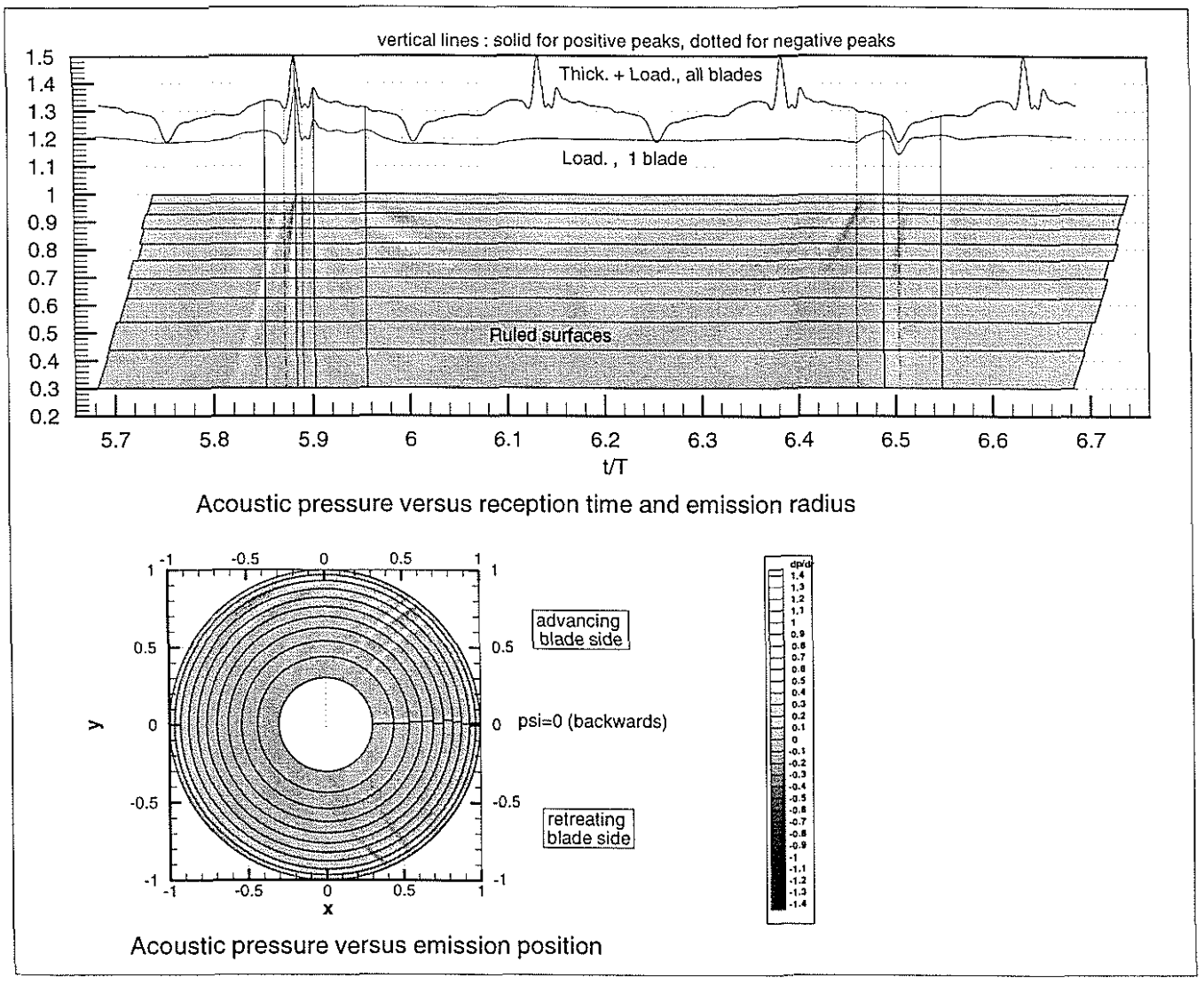

Fig. 15. Analysis of the acoustic signature construction. Baseline case. Microphone 120 m below the rotor, 150 m upstream.

The bottom of Fig. 15 presents the same ruled surface but on the rotor disk. It is reminded that the emission azimuth is found starting from the reception time using the leading edge source model. The azimuth plotted is the one of the quarter chord point. The interactions on the advancing side appear as a small negative peak followed by a higher positive peak, whereas on the retreating side the signs are inverted.

Resulting information

Let us analyze Fig. 15. The sharpest positive peak on the signatures is obviously due to the strongest interaction on the advancing side, which can be easily recognized on the rotor disk. The acoustic pressure emission is high for each blade section, and all these contributions arrive in phase at the microphone (vertical white trace on the top view). Note that this interaction is not the most parallel one on the rotor disk, and that a non parallel interaction can lead to a constructive interference effect on signatures at some microphone positions. The previous interaction, more on the left on top view, does not appear on the signature because the contributions of all sections arrive out of phase at the microphone (oblique gray trace). The interaction following the strongest one is weak but the section contributions arrive in phase on the microphone and result in a peak half as high as the highest one. Other interactions on advancing side are weak and rubbed out on signatures by destructive interferences.

The retreating side interactions can be analyzed on the right part of the top view. Only one of them leads to a negative peak on the signatures, at this microphone position. It is due to the second interaction (dark trace) on the rotor disk, following the counter-clockwise rotation. The previous interaction is stronger (darker on plots) but is totally rubbed out on the signature by destructive interference. Without IESI, the signatures would have presented several negative peaks in this area, leading to the wrong conclusion that this interaction is noisy at this microphone position.

Note that the ruled surface plots allow to see which spanwise extents are the noisiest for each interaction. The effect of tip sweep is not visible in this rectangular blade case. A sweptback tip results in small changes on the rotor disk view, but in a clearly visible shift to the right of the top of the interaction traces on the top view. This leads sometimes to more destructive interference but sometimes also to more constructive ones, all this being visible on plots like Fig. 15.

A theoretical study of the effect of sweep of a two bladed rotor on acoustic signature construction was performed starting from the blade shape of the two-bladed AH1-OLS rotor (described in [15]), and neglecting the effect of the planform modifications on the vortex characteristics (Fig. 16). A noise reduction of 4 dBA was predicted in the maximum noise directions.

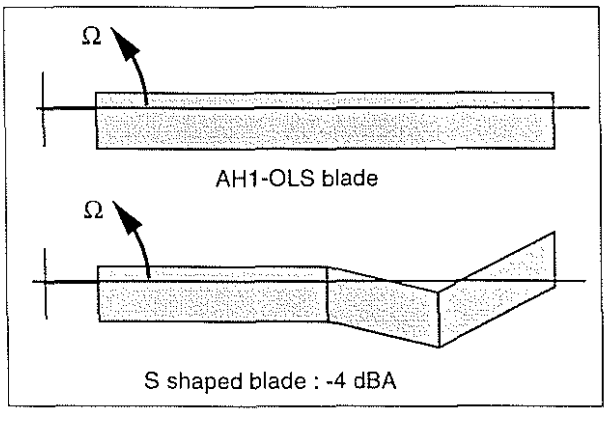

Fig. 16. Theoretical sweep modification for BVI noise reduction.

Applications

The possibility of identifying the noisiest interactions was used to choose which vortices to measure by LDV during the HART tests [4].

The present BVI analysis method was used more systematically for the ERATO aeroacoustic rotor optimization [16], cooperation between ONERA, DLR and Eurocopter, in order to identify the noisiest predicted vortices and the effect of blade sweep. It is also currently used at Eurocopter where the BVI noise prediction tools developed at ONERA [17] are implemented.

More generally, this method is often useful when noise predictions are performed for noise reduction purposes. It has therefore many fields of application including the noise predictions using measured blade pressure data.

5. CONCLUSION

The initial objective of this study was to improve the efficiency of acoustic predictions of helicopter rotor BVI noise, in order to reduce the aerodynamic and acoustic computation costs in view of low noise rotor optimization.

An Iso Event Spanwise Interpolation (IESI) method was developed. From the analysis of the acoustic signatures emitted by each computed spanwise section of the blade, it deduces the BVI geometry on the rotor disk and recreates at the observer position the effect of the physical continuity of the interactions along the blades. Artificial spurious peaks in computed signatures are avoided in low noise areas making a prediction with 10 computation sections as reliable as with 30. The amount of required pressure data is reduced in the same ratio, allowing a reduction of computer time of the aerodynamic code providing the blade pressures. As predictions with less than 10 sections are still quite accurate, the method can be used to perform noise predictions using measured blade pressures with a reasonable number of sensors. This opens new possibilities for predictions of acoustics starting from blade pressures measured in wind tunnels (even if these tunnels are not anechoic) or in flight, to serve for optimization of noise abatement flight procedures, for instance.

A tool derived from the analysis made on the blade sections signatures permits to locate on the rotor disk, azimuthally and radially, the interactions responsible for each pressure peak on the whole rotor signature. It permits to vizualize the noise signature construction mechanisms and therefore to understand why the strongest interaction at the emission are not necessarily the strongest at the reception. In particular the constructive or destructive interferences are made obvious. Hence, the effect of blade sweep can be well assessed. These possibilities are very helpful to guide low noise rotor design.

Improvements of the IESI for BVI noise predictions are still possible, like a better taking into account of the vortex curvature in case very few sections are used. However, the principle itself is very robust and could even be generalized to other applications like, for example, the High Speed Impulsive Noise predictions.

ACKNOWLEDGEMENTS

The author thanks all members of the HART cooperation, as well those from the Test Team for the high quality database made available, as those from the Prediction Team whose cooperation led to the improvement and validation of BVI prediction codes.

Particular thanks go to K. Brentner and C. Burley, from the NASA Langley Research Center, for their approval that the unpublished WOPWOP/PARIS comparisons be mentioned here.

This work has been conducted with the support of French Ministry of Defence DRET and of French Civilian Aircraft General Delegation DGAC.

REFERENCES

[1] Schultz, K.-J., Splettstoesser, W. R., « Prediction of Helicopter Rotor Impulsive Noise Using Measured Blade Pressures », 43rd Annual Forum and Technology Display, AHS, St-Louis, Missouri, USA, May, 1987.

[2] Spiegel, P., « Prévision et analyse du bruit émis par un rotor principal d'hélicoptère en présence d'interactions pale-tourbillon » (Prediction and analysis of the noise emitted by a main rotor of a helicopter in case of BVI), ONERA publication no 1996-1, February 1996, and also Thesis defended at Université du Maine, Le Mans, France, July, 1995.

[3] Spiegel, P., and Rahier, G., « Theoretical Study and Prediction of BVI Noise Including Close Interactions », AHS Technical Specialists Meeting on Rotorcraft Acoustics and Fluid Dynamics, Philadelphia, PA, USA, October 15-17, 1991.

[4] Splettstoesser, W. R., Kube, R., Wagner, W., Seelhorst, U., Boutier, A., Micheli, F., Mercker, E., and Pengel, K., « Key Results from a Higher Harmonic Control Aeroacoustic Rotor Test (HART) », Journal of the American Helicopter Society, Vol. 42, No. 1, January, 1997.

[5] Gallman, J. M., Schultz, K.-J., Spiegel, P., Burley, C. L., « Effect of Wake Structure on Blade-Vortex Interaction Phenomena : Acoustic Prediction and Validation », Journal of Aircraft, Vol. 35, No 2, March-April, 1998.

[6] Brentner, K. S., « Prediction of Helicopter Rotor Discrete Frequency Noise - A computer program incorporating realistic blade motions and advanced acoustic formulation », NASA Technical Memorandum 87721, October, 1986.

[7] Farassat, F., « Advanced Theoretical Treatment of Propeller Noise », Von Karman Institute for Fluid Dynamics lecture series 1982-08 « Propeller Performance and Noise », Rhode Saint Genèse, Belgium May 24-28, 1982.

[8] Rahier, G., and Prieur, J., « An Efficient Kirchhoff Integration Method for Rotor Noise Predicition Starting from Subsonically or Supersonically Rotating Meshes », 53rd Annual Forum of the AHS, Virginia Beach, Virginia, April 29 - May 1, 1997.

[9] Beaumier, P., and Spiegel, P., « Validation of ONERA Aeroacoustic Prediction Methods for Blade-Vortex Interaction using HART Tests Results », 51st Annual Forum and Technology Display, AHS, Fort Worth, TX, USA, May 9-11, 1995.

[10] Arnaud, G., and Beaumier, P., « Validation of R85/METAR on Puma RAE flight Tests », 18th European Rotorcraft Forum, Avignon, France, September, 1992.

[11] Michéa, B., Desopper, A., and Costes, M., « Aerodynamic Rotor Loads Prediction Method with Free Wake for Low Speed Descent Flight », 18th European Rotorcraft Forum, Avignon, France, September, 1992.

[12] Rahier, G., and Delrieux, Y., « Blade-Vortex Interaction Noise Prediction Using a Rotor Wake Roll-Up Model », Journal of Aircraft, Vol. 34, No 4, pp. 522-530, July-August, 1997.

[13] Rahier, G., « Modélisation de l'interaction profil-tourbillon en fluide parfait et application au rotor d'hélicoptère », La Recherche Aérospatiale, Vol. 3, May 1995, *including an abridged English version.*

[14] Brentner, F. S., Marcolini, M. A., and Burley, C. L, « Sensitivity of Acoustic Predictions to Variation of Input Parameters », AHS Technical Specialists Meeting on Rotorcraft Acoustics and Fluid Dynamics, Philadelphia, PA, USA, October 15-17, 1991.

[15] Splettstoesser, W. R., Schultz, K. J., Boxwell, D. A., and Schmitz, F. H., « Helicopter Model Rotor-Blade Vortex Interaction Impulsive Noise: Scalability and parametric variations », 10th European Rotorcraft Forum, The Hague, The Netherlands, September, 1984.

[16] Delrieux, Y., Prieur, J., and Declerck, D., « Aeroacoustic Prediction Tools for Quiet Rotor Design and Optimization at ONERA », AHS Aeromechanics Specialists Conference, San Francisco (CA), January 19-21, 1994.

[17] Arnaud, G., Falchéro, D., Estival, Y., and Martin, P., « Simulation of Dauphin DGV Noise in Descent Flight », Paper No AIAA-98-2237, 4th AIAA/CEAS Aeroacoustics Conference, Toulouse, France, June 2-4, 1998.